The effect of Nb addition on the thermal property, microstructure and magnetic property of FeCoZrB alloys

W. Q. YU, Y. M. SUN, Y. D. LIU, J. LIU, B. ZUO, L. H. LIU, L. R. DONG, Z. HUA*
Key Laboratory of Functional Materials Physics and Chemistry of the Ministry of Education, Jilin Normal University, Siping 136000, Jilin, P.R. China

The thermal property, microstructure and magnetic property of $Fe_{81-x}Co_xZr_{9-y}Nb_yB_{10}$ (x=2, 4, 6; y=0, 2) alloys were investigated by differential thermal analysis (DTA), X-ray diffraction (XRD) and vibrating sample magnetometer (VSM). Nb addition increases the first crystallization peak temperature. The α-Fe(Co) and α-Mn type phases are detected in the Nb-free alloys annealed at 600 °C. Only α-Fe(Co) phase is detected in the Nb-containing alloys annealed at 600 °C. Nb addition changes the crystallization processes. Abruptly deteriorations of coercivity (H_c) in the Nb-free alloys at 600 °C are observed and not found in the Nb-containing alloys. Nb addition improves H_c.

(Received December 31, 2011; accepted February 20, 2012)

Keywords: Microstructure, Thermal analysis, Magnetic

1. Introduction

Over the past several decades, research interest in Fe-based amorphous and nanocrystalline soft magnetic alloys has dramatically increased. Considerable attention is devoted to the crystallization behavior and magnetic property of Fe-based alloys [1-17]. Three main series nanocrystalline soft magnetic alloys are well established. Finemet alloy ($Fe_{73.5}Si_{13.5}B_9Nb_3Cu_1$) [14], Nanoperm alloy [FeMB (M = Nb, Zr, Hf)][15] and Hitperm alloy (FeCoMBCu) [16] have been reported one after another. Hitperm alloys have higher Curie temperatures of the residual phase, resulting in potential applications at higher operating temperatures [17]. They exhibit excellent soft magnetic properties after being annealed under optimal conditions, when they reach a nanocrystalline microstructure characterized by a nanometric α-Fe(Co) phase surrounded by a residual amorphous matrix.

Fe-based amorphous alloys crystallize through two distinct stages generally [4-6]. The first stage is the formation of b.c.c. α-Fe phase and the second stage is the formation of intermetallic compound. Moreover, the α-Mn type phase was observed in the crystallization processes of some Fe-base alloys [8-13]. The α-Mn type phase is metastable and transforms to α-Fe phase during thermal crystallization [8, 9].

In this paper, $Fe_{81-x}Co_xZr_{9-y}Nb_yB_{10}$ (x=2, 4, 6; y=0, 2) alloys are prepared. The effect of Nb addition on the thermal property, microstructure and magnetic property of FeCoZrB alloys are studied. The properties of Nb-free and Nb-containing alloys are very different.

2. Experimental details

$Fe_{81-x}Co_xZr_{9-y}Nb_yB_{10}$ (x=2, 4, 6; y=0, 2) alloys were prepared by melt-spinning and annealed at 300, 530, 600, 670 and 750 °C for 40min. The thermal analysis was investigated by differential thermal analysis (DTA, TG/DTA-6300). The microstructure was examined by X-ray diffraction (XRD, D/max 2500/PC, Cu-Kα, λ=1.5406Å). Magnetic property was measured by vibrating sample magnetometer (VSM, Lake Shore M7407).

3. Results and discussion

Fig. 1 shows the XRD patterns of $Fe_{81-x}Co_xZr_{9-y}Nb_yB_{10}$ (x=2, 4, 6; y=0, 2) alloys as-quenched. No crystalline peaks are observed, which indicates that the alloys as-quenched all form amorphous. Fig. 2 shows the DTA traces of $Fe_{81-x}Co_xZr_{9-y}Nb_yB_{10}$ (x=2, 4, 6; y=0, 2) alloys at a heating rate of 20 °C/min. When adding Nb element to FeCoZrB alloys, a low exothermic peak precedes the main crystallization peak. It is supposed to be a pre-crystallization effect [18, 19]. The first crystallization peaks T_{p1} (the main crystallization peak of the Nb-containing alloys is considered for the first crystallization peak in Table 1) and the span ΔT_p (difference between Nb-free and Nb-containing alloys) are listed in Table 1. Nb addition increases the first crystallization peak temperature. It should be related to that Nb has higher melting point than that of Zr. The degree of the temperature increase in the alloy with 6 at% Co is the maximum. For the Nb-free alloys [Fig. 2(a)], T_{p1}

decreases with increasing Co content. For the Nb-containing [Fig. 2(b)], T_{p1} decreases first and then increases.

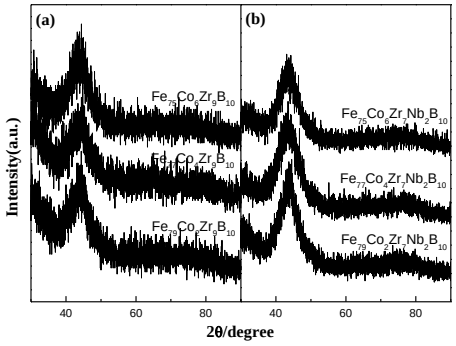

Fig. 1. XRD patterns of $Fe_{81-x}Co_xZr_{9-y}Nb_yB_{10}$ (x=2, 4, 6; y=0, 2) alloys as-quenched; (a) Nb-free alloys; (b) Nb-containing alloys.

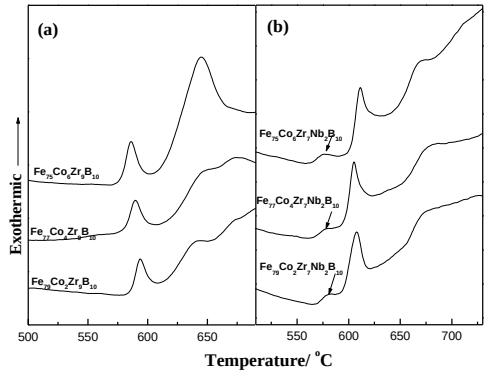

Fig. 2. DTA traces of $Fe_{81-x}Co_xZr_{9-y}Nb_yB_{10}$ (x=2, 4, 6; y=0, 2) amorphous alloys at a heating rate of 20 °C/min (a) Nb-free alloys; (b) Nb-containing alloys.

Table 1. The first crystallization peak T_{p1} and the span ΔT_{p1} of $Fe_{81-x}Co_xZr_{9-y}Nb_yB_{10}$ (x=2, 4, 6; y=0, 2) alloys.

	T_{p1}(°C)		ΔT_{p1}(°C)
	y=0	y=2	
x=2	593.9	609.8	15.9
x=4	589.4	605.1	15.7
x=6	585.8	611.2	25.4

XRD patterns of $Fe_{79}Co_2Zr_9B_{10}$ and $Fe_{79}Co_2Zr_7Nb_2B_{10}$ alloys corresponding to different annealing temperatures are shown in Fig. 3. After annealing at 300 °C, two alloys are still amorphous. After annealing at 600 °C, some crystalline phases precipitate from the amorphous matrix. It can be confirmed that the precipitated phases are bcc α-Fe and α-Mn type phases in $Fe_{79}Co_2Zr_9B_{10}$ alloy and bcc α-Fe(Co) phase in $Fe_{79}Co_2Zr_7Nb_2B_{10}$ alloy. For $Fe_{79}Co_2Zr_9B_{10}$ alloy, further increase of annealing temperature leads to the α-Mn type phase transforms to α-Fe phase. The α-Fe(Co), Fe_3Zr and $ZrFe_2$ phases are observed at the final crystallization stage. The crystallization processes of $Fe_{81-x}Co_xZr_{9-y}Nb_yB_{10}$ (x=4, 6; y=0) alloys are similar as $Fe_{79}Co_2Zr_9B_{10}$ alloy. XRD patterns of Nb-free alloys annealed at 600 °C are shown in Fig. 4(a). For $Fe_{79}Co_2Zr_7Nb_2B_{10}$ alloy, further increase of annealing temperature leads to the increase of the intensity of α-Fe(Co) diffraction peaks and the increase of grain size [α-Fe(Co)]. The grain size [α-Fe(Co)] of the alloys annealed at 530, 600, 670 and 750 °C is 17.5, 18.1, 20.4 and 28.1nm, respectively. The crystallization processes of $Fe_{81-x}Co_xZr_{9-y}Nb_yB_{10}$ (x=4, 6; y=2) alloys are similar as $Fe_{79}Co_2Zr_7Nb_2B_{10}$ alloy [19]. XRD patterns of Nb-containing alloys annealed at 600 °C are shown in Fig. 4(b). Nb addition changes the crystallization processes.

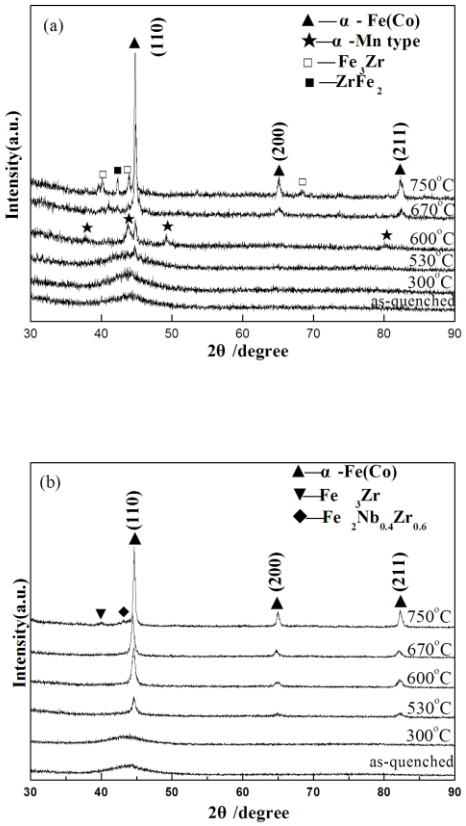

Fig. 3. XRD patterns of $Fe_{79}Co_2Zr_9B_{10}$ and $Fe_{79}Co_2Zr_7Nb_2B_{10}$ amorphous alloys as-quenched and annealed at different annealing temperatures (a) $Fe_{79}Co_2Zr_9B_{10}$; (b) $Fe_{79}Co_2Zr_7Nb_2B_{10}$.

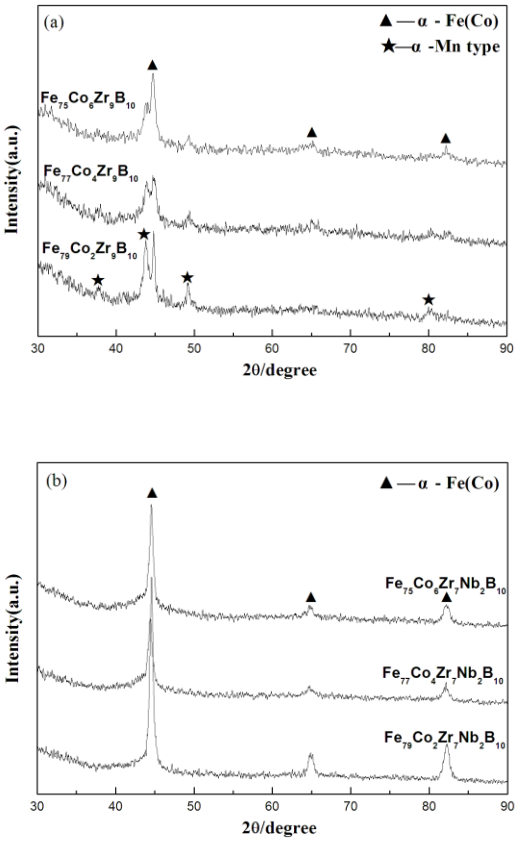

Fig. 4. XRD patterns of $Fe_{81-x}Co_xZr_{9-y}Nb_yB_{10}$ (x=2, 4, 6; y=0, 2) alloys annealed at 600 °C (a) Nb-free alloys; (b) Nb-containing alloys.

Fig. 5 shows the coercivity ($\boldsymbol{H_c}$) of $Fe_{81-x}Co_xZr_{9-y}Nb_yB_{10}$ (x=2, 4, 6; y=0, 2) alloys as a function of annealing temperature (T_a). It is well known that magnetic properties of a ferromagnetic material are closely related to its microstructure. The variations of $\boldsymbol{H_c}$ in the Nb-free alloys are similar. $\boldsymbol{H_c}$ increases slowly at 530 °C and abruptly deteriorates at 600 °C. The deterioration of $\boldsymbol{H_c}$ is related to the precipitation of α-Mn type phase. It maybe that α-Mn type phase has large magnetocrystalline anisotropy. The observed magnetic softening later is due to the disappearence of α-Mn type phase and the stronger exchange coupling between bcc α-Fe(Co) nanocrystals. An increase in the $\boldsymbol{H_c}$ observed at 750 °C is assumed to the precipitation of Fe_3Zr etc. phases. The variations of $\boldsymbol{H_c}$ in the Nb-containing alloys are similar. $\boldsymbol{H_c}$ decreases to the minimum value at 530 °C, which is related to the release of the residual stresses and structure relaxation of the amorphous phase. Above 600 °C, $\boldsymbol{H_c}$ increases continuously, which is due to the increase of grain size [α-Fe(Co)]. A rapid increase in the $\boldsymbol{H_c}$ observed at 750 °C is assumed to the precipitation of Fe_3Zr etc. phases. $\boldsymbol{H_c}$ and the span $\Delta\boldsymbol{H_c}$ (difference between Nb-free and Nb-containing alloys) of $Fe_{81-x}Co_xZr_{9-y}Nb_yB_{10}$ (x=2, 4, 6; y=0, 2) alloys annealed at 600 °C are listed in Table 2. Nb addition improves $\boldsymbol{H_c}$ of alloys. The degree of the improvement of $\boldsymbol{H_c}$ in the alloy with 4at% Co is the maximum.

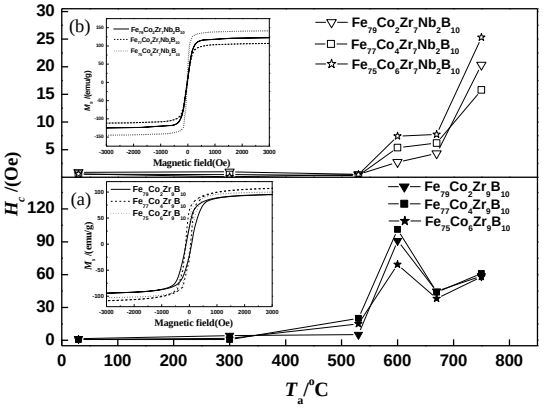

Fig. 5. $\boldsymbol{H_c}$ of $Fe_{81-x}Co_xZr_{9-y}Nb_yB_{10}$ (x=2, 4, 6; y=0, 2) alloys as a function of annealing temperature (T_a). The insets show the magnetic hysteresis loops of $Fe_{81-x}Co_xZr_{9-y}Nb_yB_{10}$ (x=2, 4, 6; y=0, 2) alloys annealed at 600 °C; a) Nb-free alloys; (b) Nb-containing alloys.

Table 2. Coercivity ($\boldsymbol{H_c}$) and the span $\Delta\boldsymbol{H_c}$ of $Fe_{81-x}Co_xZr_{9-y}Nb_yB_{10}$ (x=2, 4, 6; y=0, 2) alloys annealed at 600 °C.

	H_c (Oe)		ΔH_c (Oe)
	y=0	y=2	
x=2	91.0	2.8	88.2
x=4	101.2	5.4	95.8
x=6	69.3	7.5	61.8

4. Conclusions

$Fe_{81-x}Co_xZr_{9-y}Nb_yB_{10}$ (x=2, 4, 6; y=0, 2) alloys as-quenched all form amorphous. The thermal property, microstructure and magnetic property between Nb-free and Nb-containing alloys are very different. A pre-crystallization effect is found in the Nb-containing alloys and not found in the Nb-free alloys. Nb addition increases the first crystallization peak temperature. The degree of the temperature increase in the alloy with 6at% Co is the maximum. The processes of $Fe_{81-x}Co_xZr_{9-y}Nb_yB_{10}$ (x=2, 4, 6; y=0) alloys are complex. The α-Fe(Co) and α-Mn type phases are detected in the Nb-free alloys annealed at 600 °C. The α-Mn type phase transforms to α-Fe phase at higher temperature. Only α-Fe(Co) phase is detected in the Nb-containing alloys annealed at 600 °C. Nb addition changes the crystallization processes of alloys. Abruptly deteriorations of $\boldsymbol{H_c}$ in the

Nb-free alloys are observed at 600 °C and not found in the Nb-containing alloys, which is related to the precipitation of α-Mn type phase. It may be that α-Mn type phase has large magnetocrystalline anisotropy. The observed magnetic softening at 670 °C is due to the disappearence of α-Mn type phase and the stronger exchange coupling between bcc α-Fe(Co) nanocrystals. H_c of the Nb-containing alloys increases continuously above 600 °C, which is due to the increase of grain size [α-Fe(Co)]. Nb addition improves H_c of alloys. The degree of the improvement of H_c in the alloy with 4at% Co is the maximum.

Acknowledgments

This work was funded by Science and Technology Development Project of Jilin Province (No. 201105083), Science and Technology Studying Project of "12th five-year" Office of Education of Jilin Province (No. 2011-158) and Graduate Innovative Research Programs of Jilin Normal University (No. 201103).

References

[1] C. Q. Zhang, Z. H. Zhang, Z. Qi, Y. X. Qi, J. Y. Zhang, X. F. Bian, J Non-Cryst. Solids **354**, 3812 (2008).
[2] A. Fernández-Martínez, P. Gorría, G. J. Cuello, J. D. Santos, M. J. Pérez, J. Non-Crys. Sol. **353**, 855 (2007).
[3] H. Huang, G. Shao, P. Tsakiropoulos, J. Alloys Compd. **459**, 185 (2008).
[4] M. Al-Haj, J. Barry, J. Mater. Sci. Lett. **17**, 1125 (1998).
[5] D. M. Zhu, K. Raviprasad, K. Suzuki, S. P. Ringer, Mater. Forum, **27**, 74 (2004).
[6] K. Suzuki, A. Makino, A. P. Tsai, A. Inoue, T. Masumoto, Mater. Sci. Eng. A **179-180**, 501 (1994).
[7] N. Randrianantoandro, I. Labaye, L. Berger, O. Crisan, M. Grafoute, F. Calvayrac J.-M. Greneche, J. Optoelectron. Adv. Mater. **4**, 193 (2002).
[8] M. Imafuku, S. Sato, H. Koshiba, E. Matsubara, A. Inoue, Scripta mater. **44**, 2369 (2001).
[9] W. Q. Yu, Y. M. Sun, Z. Hua, Applied Surface Science **257**, 9733 (2011).
[10] I. V. Lyasotskii, N. B. Dyakonova, E. N. Vlasova, D. L. Dyakonov, M. Yu. Yazvitskii, Physica status solidi (a) **203**, 259 (2006).
[11] I. V. Lyasotskii, N. B. Dyakonova, E. N. Vlasova, D. L. Dyakonov, B. V. Molotilov, Bull. Russ Acad Sci, Phys. **65**, 1549 (2001).
[12] I. V. Lyasotskii, N. B. Dyakonova, D. L. Dyakonov, E. N. Vlasova, M. Yu. Yazvitskii, Rev. Adv. Mater. Sci. **18**, 695 (2008).
[13] T. Nagase, Y. Umakoshi, ISIJ International, **46**, 1371 (2006).
[14] Y. Yoshizawa, S. Oguma, K. Yamauchi, J Appl. Phys. **64**, 6044 (1988).
[15] K. Suzuki, A. Makino, N. Kataoka, A. Inoue, T. Masumoto, Mater. Trans. JIM **32**, 93 (1991).
[16] M. A. Willard, D. E. Laughlin, M. E. McHenry, D. Thoma, K. Sickafus, J. O. Cross, V. G. Harris, J. Appl. Phys. **84**, 6773 (1998).
[17] Y. Sun, L. Zhong, X. F. Bi, Scripta Materialia, **60**, 814 (2009).
[18] E. Illeková, P. Švec, M. Miglierini, J. Non-Cryst. Sol. **353**, 3342 (2007).
[19] W. Q. Yu, Y. M. Sun, L. H. Liu, L. R. Dong, Z. Hua, Acta Physica Polonica A. **120**, 1034 (2011).

*Corresponding author: huazhong196110@163.com